Dalton Transactions

PAPER

View Article Online
View Journal | View Issue

Cite this: *Dalton Trans.*, 2015, **44**, 14896

cis-Pt $I_2(NH_3)_2$: a reappraisal†

Tiziano Marzo,[a] Serena Pillozzi,[b] Ondrej Hrabina,[c] Jana Kasparkova,[d] Viktor Brabec,[d] Annarosa Arcangeli,[b] Gianluca Bartoli,[b] Mirko Severi,[e] Alessandro Lunghi,[e] Federico Totti,[e] Chiara Gabbiani,[f] Adóracion G. Quiroga[g] and Luigi Messori*[a]

Received 26th March 2015,
Accepted 17th July 2015

DOI: 10.1039/c5dt01196e

www.rsc.org/dalton

The investigation of *cis*-$PtI_2(NH_3)_2$, the diiodido analogue of cisplatin (*cisPtI*$_2$ hereafter), has been unjustly overlooked so far mainly because of old claims of pharmacological inactivity. Some recent – but still fragmentary – findings prompted us to reconsider more systematically the chemical and biological profile of *cisPtI*$_2$ in comparison with cisplatin. Its solution behaviour, interactions with DNA and cytotoxic properties *versus* selected cancer cell lines were thus extensively analysed through a variety of biophysical and computational methods. Notably, we found that *cisPtI*$_2$ is highly cytotoxic *in vitro* toward a few solid tumour cell lines and that its DNA platination pattern closely reproduces that of cisplatin; *cisPtI*$_2$ is also shown to completely overcome resistance to cisplatin in a platinum resistant cancer cell line. The differences in the biological actions of these two Pt complexes are most likely related to slight but meaningful differences in their solution behaviour and reactivity. Overall, a very encouraging and unexpected pharmacological profile emerges for *cisPtI*$_2$ with relevant implications both in terms of mechanistic knowledge and of prospective clinical application. An *ab initio* DFT study is also included to support the interpretation of the solution behaviour of *cisPtI*$_2$ under physiological and slightly acidic pH conditions.

Introduction

Cisplatin is a leading compound in the field of anticancer drugs. Together with its two main parent Pt drugs, *i.e.* carboplatin and oxaliplatin, it is currently used in about half of chemotherapeutic protocols for cancer treatment.[1–3] Since the discovery of its outstanding anticancer properties during the 60s and subsequent clinical approval by FDA, in 1978, cisplatin has been the subject of hundreds of studies to describe and understand its peculiar chemical behaviour, and elucidate the mechanisms of its biological and pharmacological effects.[4–6]

A quite wide consensus now exists concerning the likely mode of action of anticancer Pt drugs that mainly relies on direct DNA damage, impairment of fundamental DNA functions and consequent triggering of apoptosis;[1,2] yet, several issues and details remain unexplored and/or unanswered, so that other mechanistic hypotheses – even DNA unrelated – have been advanced.[7,8]

The great clinical success of cisplatin has inspired an intense search for platinum analogues with hopefully improved biological and pharmacological properties;[9–13] however, the outcomes of these research activities turned out to be quite modest and disappointing, both in terms of identification of new clinically effective Pt agents and discovery of innovative modes of action.

Despite the huge research efforts made on platinum analogues over the last three decades, we were surprised on learning that only rare studies were carried out on *cisPtI*$_2$, the strict iodo analogue of cisplatin (Fig. 1). This is probably the consequence

Fig. 1 Structure of cisplatin and its diiodido analogue.

[a]*MetMed, Department of Chemistry, University of Florence, Via della Lastruccia 3, 50019 Sesto Fiorentino, Italy. E-mail: luigi.messori@unifi.it*
[b]*Department of Experimental and Clinical Medicine, University of Florence, Viale GB Morgagni 50, 50134 Firenze, Italy*
[c]*Department of Biophysics, Faculty of Science, Palacky University, Slechtitelu 11, CZ-78371 Olomouc, Czech Republic*
[d]*Institute of Biophysics, Academy of Sciences of the Czech Republic, v.v.i., Kralovopolska 135, CZ-61265 Brno, Czech Republic*
[e]*Department of Chemistry "Ugo Schiff", University of Florence, Via della Lastruccia, 3, 50019 Sesto Fiorentino, Firenze, Italy*
[f]*Department of Chemistry and Industrial Chemistry, University of Pisa via Moruzzi, 3, 56124 Pisa, Italy*
[g]*Department of Inorganic Chemistry, Universidad Autonóma de Madrid C/Francisco Tomás y Valiente 7, 28049 Madrid, Spain*

†Electronic supplementary information (ESI) available: UV-Vis spectrum of complex *cis*-$Pt(NH_3)_2I_2$ × 10^{-4} M in the presence of KI, kinetic studies, ESI MS experiments, DNA interstrand cross-linking in the linear pUC19 DNA, DNA unwinding. See DOI: 10.1039/c5dt01196e

of an initial negative assessment by Hoeschele and Cleare,[14a] who reported that *cisPtI*$_2$ is nearly inactive in animal models of sarcoma 180 while warning about its extremely low aqueous solubility and the difficulty in determining the toxic dose. Accordingly, even the cytotoxicity profile of *cisPtI*$_2$ against the 60 cancer cell lines panel of NCI has never been reported.

However, more recently, a few studies started reconsidering iodido platinum complexes as possible anticancer drug candidates. For instance, Kratochwil *et al.*, described some diamino diiodido platinum(II) complexes manifesting an appreciable cytotoxicity *in vitro*.[15] In the last few years, we discovered that some mixed diamino diiodido Pt complexes exhibit appreciable cytotoxic properties *in vitro*.[16–18] Moreover, for some of these Pt complexes, in spite of their lower reactivity with DNA as compared to cisplatin, an unconventional reactivity toward the model protein cytochrome *c* was disclosed, unexpectedly characterized by the loss of the amino ligands and retention of the iodido ligands.[16,17] Furthermore, in a paper published in 2013, we structurally described the reaction of *cisPtI*$_2$ with lysozyme, confirming the peculiar and different interaction mode toward this model protein in comparison with cisplatin.[19] Yet, no study has re-evaluated so far the biological profile of *cisPtI*$_2$. Altogether, these arguments led us to reconsider, in a more systematic way, some key chemical and biological aspects of *cisPtI*$_2$ with respect to cisplatin.

Specifically, we have focused our attention on the following four issues: (i) the activation process of *cisPtI*$_2$ in aqueous solutions both at physiological and slightly acidic pH; (ii) a computational rationalization of the spectral results; (iii) the investigation of the direct reaction of *cisPtI*$_2$ with DNA; (iv) the cellular effects of *cisPtI*$_2$ in a small panel of cancer cell lines. Some notable results have emerged from these studies that are comprehensively analysed and discussed here in direct comparison with cisplatin, with relevant mechanistic and medical implications.

Experimental

Chemistry of *cis*-$PtI_2(NH_3)_2$

Synthesis of *cis*-$PtI_2(NH_3)_2$ and UV-Vis analysis. *cisPtI*$_2$ was synthesized according to published procedures, using (1 : 4) Pt : KI in order to avoid further purifications.[17,20] The purity of the product was checked by elemental analysis of C, N and H [calculated C: 0%, H: 1.26%, N: 5.84%, experimental: C: 0%, H: 1.12%, N: 5.71%], and as described in ref. 14*b*. The correct *cis* geometry was assessed by comparison with its *trans* analogue as describe in the literature.[14] Solution behaviour of *cisPtI*$_2$ was assessed through spectrophotometric studies performed with a Varian Cary 50 Bio UV-Vis spectrophotometer in buffered solutions without the use of DMSO and in the absence of NaCl. A solution of the complex (10^{-4} M) was prepared in 50 mM phosphate buffer (with or without the presence of KI) at pH = 7.4 or in 20 mM ammonium acetate buffer at pH = 4.5 and the absorbance was monitored in the wavelength range between 200 and 800 nm for 72 h at 25° C.

Density functional theory simulations. ORCA package has been used throughout the calculations.[21] Hybrid PBE0 functional[22] and Aldrich TZVP Gaussian basis sets with scalar relativistic (ZORA) corrections[23] were used for both geometry optimizations and spectra simulations. Excited states have been computed within the TDDFT approach[24] and only the first twenty transitions have been computed using 200 expansion vectors in the iterative solution of the CI equations. D3 Grimme's dispersion corrections[25] have also been included. Solvent effects have been taken into account within the COSMO model[26,27] with an ε value of 80.4. Highly accurate integration grids (Grid 5 in the ORCA notation) without pruning of the inner angular part of the wave function and "TightSCF" convergence criteria have been used throughout all the calculations.

Log *P* determination. The octanol–water partition coefficients for cisplatin and *cisPtI*$_2$ were determined by modification of the reported shake flask method.[28] Water (50 mL, distilled after Milli-Q purification) and *n*-octanol (50 mL) were shaken together for 72 h to allow saturation of both phases. Solution of the complexes were prepared in the aqueous phase (3×10^{-3} M) and an equal volume of octanol was added. Biphasic solutions were mixed for ten minutes and then centrifuged for five minutes at 6000 rpm to allow separation. Concentration in both phases was determined by UV-VIS. Reported log *P* is defined as $\log[\text{complex}]_{oct}/[\text{complex}]_{wat}$. Final values were reported as the mean of three determinations.

Uptake experiment: comparison between cisplatin and *cis*-$PtI_2(NH_3)_2$ HCT116 cell line. The determination of platinum concentration in the cellular pellets as well as in the corresponding supernatant samples was performed in triplicate by a Varian 720-ES Inductively Coupled Plasma Atomic Emission Spectrometer (ICP-AES) equipped with a CETAC U5000 AT+ ultrasonic nebulizer, in order to increase the method sensitivity. Before the analysis, samples were weighed in PE vials and digested in a thermo-reactor at 80 °C for 24 h with 2 mL of *aqua regia* (HCl suprapure grade and HNO_3 suprapure grade in 3 : 1 ratio) and 0.2 mL of H_2O_2 suprapure grade. After digestion, the samples were diluted to about 5 mL with ultrapure water (≤18 MΩ) and accurately weighed; 5.0 mL of each sample were spiked with 1 ppm of Ge used as an internal standard and analysed. Calibration standards were prepared by gravimetric serial dilution from a commercial standard solution of Pt at 1000 mg L^{-1}. The wavelength used for Pt determination was 214.424 nm whereas for Ge the line at 209.426 nm was used. The operating conditions were optimized to obtain maximum signal intensity, and between each sample, a rinse solution of HCl suprapure grade and HNO_3 suprapure grade in 3 : 1 ratio was used in order to avoid any "memory effect".

Cellular studies

Cell cultures. PANC-1, HCT116-S, HCT116-R, IGROV-1, A549 and HT29 cell lines were cultured in RPMI 1640 (Euroclone; Milan, Italy) with 10% Fetal Bovine Serum (FBS) (Euroclone Defined; Euroclone; Milan, Italy). HCT116 cells were kindly

provided by Dr R. Falcioni (Regina Elena Cancer Institute, Roma). We cultured the cell lines at 37 °C under a humidified atmosphere in 5% CO_2 in air.

Pharmacology experiments. Cells were seeded in a 96-well flat-bottomed plate (Corning-Costar, Corning, NY, USA) at a cell density of 1×10^4 cells per well in RPMI complete medium. Drugs were used, after solubilisation in water, without using DMSO, at the final concentrations indicated in the figures and in the legends to the figures. After 24 h, viable cells (determined by Trypan blue exclusion) were counted in triplicate using a haemocytometer. Each experimental point represents the mean of four samples carried out in three separate experiments.

Trypan blue assay. Cells viability was assessed by the Trypan blue exclusion assay. In brief, 10 μL of 0.4% trypan blue solution was added to 10 μL cell suspensions in culture medium.

The suspension was gently mixed and transferred to a haemocytometer. Viable and dead cells were identified and counted under a light microscope. Blue cells failing to exclude the dyes were considered nonviable, and transparent cells were considered viable. The percentage of viable cells was calculated on the basis of the total number of cells (viable plus nonviable). The IC_{50} value (*i.e.*, the dose that caused apoptosis of 50% of cells) was calculated by fitting the data points (after 24 h of incubation) with a sigmoidal curve using Calcusyn software.

Cell cycle analysis. The effect of cisplatin and *cisPtI*$_2$ on cell cycle distribution was assessed by flow cytometry after staining the cells with propidium iodide (PI). Briefly, the cells (5×10^5 cells per mL) were analyzed prior to and after treatment with IC_{50s} of both drugs (20.98 μM and 7.3 μM) for 24 h. The cells were harvested, washed with PBS and resuspended in 300 μL 1× propidium iodide staining solution and incubated at 4 °C in the dark for 20 minutes. DNA content of the cells was measured by BD FACSCanto Flow Cytometer and the population of each phase was determined using ModFit LT 3.0 analysis software (Verity Software House, Topsham, ME USA).

DNA binding studies

Reaction of *cisPtI*$_2$ with DNA, its putative main target, was analysed in direct comparison with cisplatin through a robust experimental approach including quantification of Pt binding to DNA, DNA interstrand cross-linking analysis, DNA adducts characterization by ethidium bromide fluorescence, DNA unwinding and thermal stability analyses.

Quantitative evaluation of binding of cis-$PtI_2(NH_3)_2$ and cisplatin to mammalian DNA in a cell-free medium. Solutions of double-helical calf thymus (CT) DNA (42% G + C, mean molecular mass approximately 2×10^7) at a concentration of 0.032 mg mL^{-1} (1×10^{-4} M related to the phosphorus content) were incubated with *cisPtI*$_2$ (8 μM) or cisplatin (8 μM) at a value of $r_f = 0.08$ in 0.1 mM KI or KCl, respectively, at 37 °C (r_f is defined as the molar ratio of free platinum complex to nucleotide phosphates at the onset of incubation with DNA). Two different stock solutions of *cisPtI*$_2$ (0.1 mM) or cisplatin (0.1 mM) were prepared. One contained the Pt^{II} complex incubated for 7 days in unbuffered KI or KCl, respectively (0.01 M, pH 6) at 37 °C in the dark, whereas the other contained Pt^{II} complexes incubated for 7 days in double distilled water at 37 °C in the dark. Fifty microliters of the Pt^{II} complex aged in KI/KCl (0.01 M) or in water were quickly mixed with 4950 μL of DNA dissolved in $NaClO_4$ (10 mM), and the reaction mixture was maintained at 37 °C. In the experiments in which the Pt^{II} complex aged in water was used, the final reaction mixture was still supplemented at the onset of the reaction with KI or KCl so that the resulting concentration of KI or KCl in the reaction mixtures was always 0.1 mM. At various time intervals, an aliquot of the reaction mixture was withdrawn and assayed by differential pulse polarography (DPP) for platinum not bound to DNA.[29]

Platination reactions. If not stated otherwise, CT or plasmid DNAs were incubated with the platinum complex in 10 mM $NaClO_4$ at 37 °C in the dark. After 24 h, the samples were exhaustively dialyzed against the medium required for subsequent biochemical or biophysical analysis. An aliquot of these samples was used to determine the value of r_b (r_b is defined as the number of molecules of the platinum complex bound per nucleotide residue) by flameless atomic absorption spectrophotometry (FAAS) or by differential pulse polarography (DPP).[29]

Unwinding of negatively supercoiled DNA. Unwinding of closed circular supercoiled pSP73KB plasmid DNA (2455 bp) was assayed by an agarose gel mobility shift assay.[30] The unwinding angle Φ, induced per platinum–DNA adduct was calculated upon the determination of the r_b value at which the complete transformation of the supercoiled to the relaxed form of the plasmid was attained. Samples of pSP73KB plasmid were incubated with platinum compounds at 37 °C in the dark for 24 h. The samples were subsequently subjected to electrophoresis on 1% agarose gels running at 25 °C with tris-(hydroxymethyl) aminomethane (Tris)-acetate–EDTA buffer. The gels were then stained with EtBr, followed by photography with a transilluminator.

DNA melting. The melting curves of CT DNAs were recorded by measuring the absorbance at 260 nm. The melting curves were recorded in a medium containing 0.1 M Na^+ with 1 mM Tris-HCl/0.1 mM Na_2H_2EDTA, pH 7.4. The value of the melting temperature (t_m) was determined as the temperature corresponding to a maximum on the first derivative profile of the melting curves.

Interstrand DNA cross-linking in a cell-free medium. *cisPtI*$_2$ or cisplatin were incubated for 24 h with 0.5 μg of a linear 2686-bp fragment of pUC19 plasmid linearized by EcoRI. The linear fragment was first 3′-end-labeled by means of the Klenow fragment of DNA polymerase I in the presence of [α-^{32}P]dATP. The platinated samples were analyzed for DNA interstrand crosslinks by previously published procedures.[31,32] The number of interstrand cross-links was analyzed by electrophoresis under denaturing conditions on alkaline agarose gel (1%). After the electrophoresis had been completed, the intensities of the bands corresponding to single strands of DNA and interstrand cross-linked duplex were quantified. The frequency

of interstrand cross-links was calculated as ICL/Pt (%) = XL/5372r_b (the DNA fragment contained 5372 nucleotide residues), where ICL/Pt (%) is the number of interstrand cross-links per adduct multiplied by 100, and XL is the number of interstrand cross-links per molecule of the linearized DNA duplex, which was calculated assuming a Poisson distribution of the interstrand crosslinks as XL = $-\ln A$, where A is the fraction of molecules running as a band corresponding to the non-cross-linked DNA.

Characterization of DNA adducts by EtBr fluorescence. These measurements were performed on a Varian Cary fluorescence spectrophotometer using a 1 cm quartz cell.

Fluorescence measurements were performed at an excitation wavelength of 546 nm, and the emitted fluorescence was analyzed at 590 nm. The fluorescence intensity was measured at 25 °C in NaCl (0.4 M) to avoid secondary binding of EtBr to DNA.[26] The concentrations were 0.01 mg mL^{-1} for DNA and 0.04 mg mL^{-1} for EtBr, which corresponded to the saturation of all intercalation sites of EtBr in DNA.[33]

Other physical methods. Absorption spectra were measured with a Beckman 7400 DU spectrophotometer equipped with a thermoelectrically controlled cell holder. The FAAS measurements were conducted with a Varian AA240Z Zeeman atomic absorption spectrometer equipped with a GTA 120 graphite tube atomizer. The gels were visualized with a FUJIFILM BAS 2500 bioimaging analyzer, and the radioactivity associated with the bands was quantified with an AIDA Image Analyzer. DPP measurements were performed using an EG&G PARC Electrochemical Analyzer, model 384B.

Results

Solution chemistry of *cis*-Pt $I_2(NH_3)_2$: log *P* determination and activation profile in aqueous buffers

We first investigated some unexplored chemical features of *cisPtI*$_2$; in particular we determined its log *P* value and analysed its solution behaviour under various conditions and the inherent metal complex activation processes.

The log *P* of *cisPtI*$_2$ was measured according to the method reported in the Experimental section; a value of −0.13 was determined *versus* a value of −2.4 previously determined for cisplatin and once again confirmed here. This result implies that *cisPtI*$_2$, in its intact form, is far more lipophylic than cisplatin: this might have some appreciable impact on its cellular uptake (see later).

Then, the solution behaviour of *cisPtI*$_2$ was studied spectrophotometrically under physiological-like or slightly acidic pH conditions. Remarkably, freshly prepared aqueous solutions of *cisPtI*$_2$, at pH = 7.4, manifest two intense bands in the UV-visible region, located at 290 and 350 nm, respectively that allow the direct and continuous monitoring of the solution behaviour of this platinum complex (Fig. 2).

Some important spectral changes are slowly detected consisting of the progressive and regular decrease of the two main bands and in the appearance of a new band, of lower intensity, around 280 nm. The observed spectral changes are tentatively traceable to the progressive release of the two iodido ligands and to their replacement by water molecules according to a moderately biphasic kinetics. This would mean that the aquation process of *cisPtI*$_2$ is quite close to that of cisplatin, involving the progressive detachment of the two halide ligands while both ammonia ligands are retained as confirmed by some further experiments. In particular, addition of KI at increasing concentrations completely eliminated and even reverted the above described spectral changes (see ESI†) strongly supporting the proposed interpretation. In any case, the rate of the aquation process for *cisPtI*$_2$ is appreciably slower than that for cisplatin (by at least a factor 2) possibly because of the greater strength of the Pt–I bond and/or greater inertness related to the increased "soft" character of iodide over chloride (more details of the hydrolysis process and UV-Vis analysis are given in the ESI†).

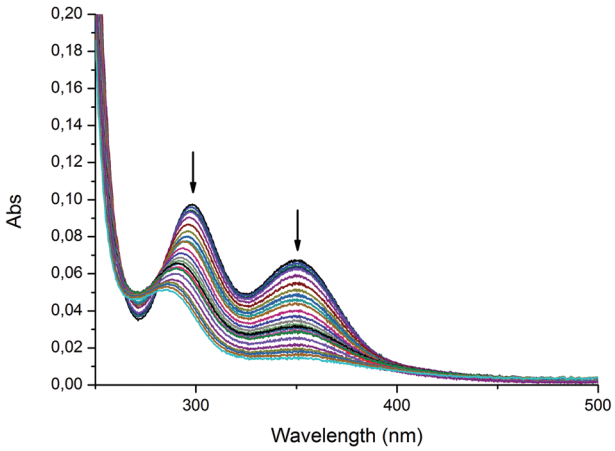

Fig. 2 Time dependent UV-Vis analysis of complex *cis*-$PtI_2(NH_3)_2$ × 10^{-4} M in 50 mM phosphate buffer (pH = 7.4) followed for 72 h.

To gain further insight into the activation processes of *cisPtI*$_2$, we also analysed its spectral behaviour under slightly acidic conditions. Indeed, a mildly acidic environment is thought to destabilise the ammonia ligands and thus favour ammonia release over iodide release. Accordingly, *cisPtI*$_2$ was dissolved in an acetate buffer, at pH 4.5, and its spectral changes were monitored over 72 hours. The resulting spectral profile is shown in Fig. 3: it is apparent that the overall spectral profile is profoundly different from that recorded at physiological pH. In particular, a new and quite intense visible band is clearly detected around 410 nm, at 72 hours, whose assignment is discussed later.

Computational studies, simulation of UV-Vis spectra

To interpret the reported spectral profiles at two distinct pH values, we performed UV-Vis spectral simulations of 5 species: the native *cisPtI*$_2$, two products of the iodido aquation mechanism *i.e.* [*cis*-$PtI(H_2O)(NH_3)_2]^+$ (**1**) and [*cis*-$Pt(H_2O)_2(NH_3)_2]^{2+}$ (**2**)

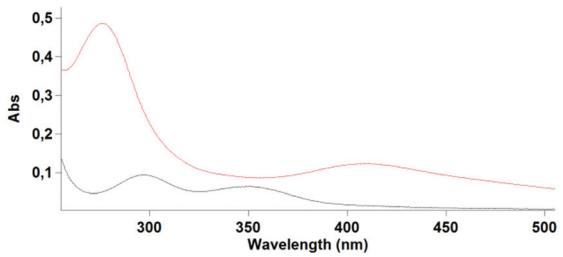

Fig. 3 UV-Vis spectral changes of complex *cis*-$PtI_2(NH_3)_2$ × 10^{-4} M in 50 mM acetate buffer (pH = 4.5) followed for 72 h. Gray line t = 0 h, red line t = 72 h.

and two products related to the ammonia aquation mechanism *i.e.* [*cis*-$PtI_2(NH_3)(H_2O)$] (**3**) and [*cis*-$PtI_2(H_2O)_2$] (**4**).

The computed spectrum of *cisPtI*$_2$ (*cf.* red line in Fig. 4a) is in very good agreement with the experimental one reported in Fig. 2. The calculated spectra for the mono- and di-iodido hydrolysis species, *i.e.* (**1**) and (**2**), are reproduced close to the experimental spectral evolution shown in Fig. 2, offering strong support to the iodide release mechanism.

Simulated band assignments were done through transition density plots reported in Fig. 4b. It is possible to observe that, for *cisPtI*$_2$, band A is a LMCT transition, I,O($p_{x,y}$) → Pt($d_{x^2-y^2}$), while band B is a platinum d–d transition, Pt(d_{xy}) → Pt($d_{x^2-y^2}$).

Notably, band A changes from a LMCT to a platinum d–d character passing from *cisPtI*$_2$ to species (**1**) and (**2**). For (**1**), both bands have a Pt(d_{xy}) → Pt($d_{x^2-y^2}$) character. For (**2**) we observed that the (B) band observed for the *cisPtI*$_2$ undergoes a blue shift until it turns into band (A).

Band B conserved the Pt(d_{xy}) → Pt($d_{x^2-y^2}$) character observed for (**2**). Such behavior is in agreement with expected d orbital shift due to the substitution of a strong basic π donor as an iodide with one water molecule.

To verify the correctness of the supposed iodide hydrolysis mechanism for physiological-like pH conditions, we have computed the UV-Vis spectra (see Fig. 5a) also for the species involved in the concurrent amino hydrolysis mechanism, *i.e.* (**3**) and (**4**). In this case, the two *cisPtI*$_2$ bands undergo a significant red shift keeping their shape and relative intensities practically unchanged. Interestingly, the same behavior is experimentally observed for acidic conditions (*cf.* Fig. 3), where, indeed, the release of the ammonia ligands is expected. Furthermore, since dimeric species of the type [Pt(amine)I_2]$_2$, that are active on selected cancer cell lines, were reported to have been synthesised under acidic conditions;[34] additional ESI MS experiments were carried out at pH = 4.5. Formation of dimers in solution under the latter conditions is confirmed by the presence of few weak peaks assignable to these species (see ESI†).

The difference transitions MOs analysis performed for (**3**) and (**4**) is shown in Fig. 5b; it is observed that the nature of the main spectral transitions is retained for all species involved. In this case, only the shift of valence molecular orbitals has been observed due to similar orbital contributions of

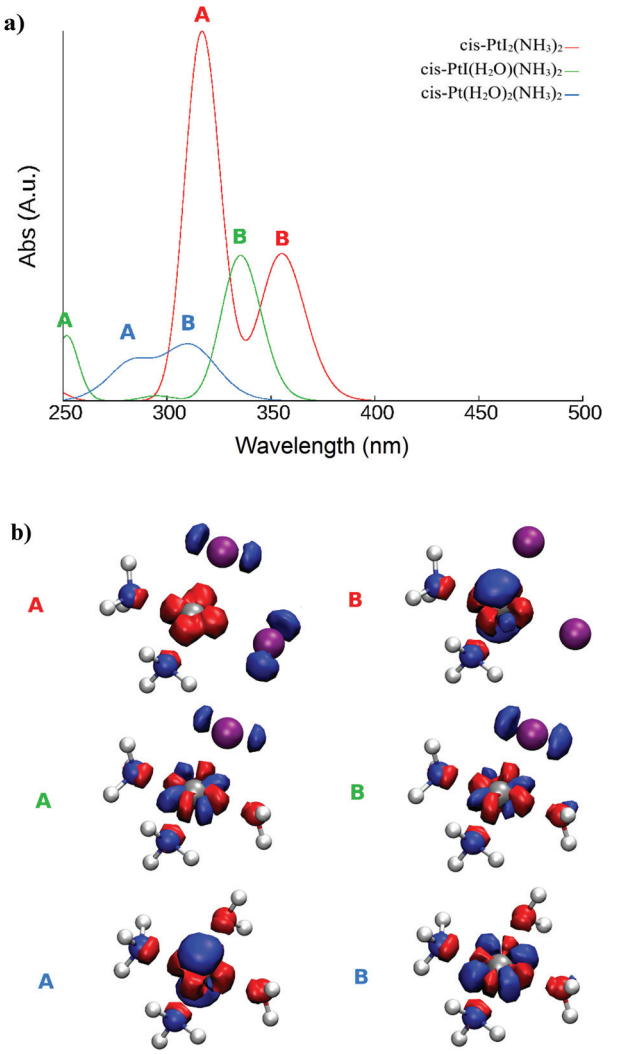

Fig. 4 (a) Evolution of UV-Vis spectral features for the iodide hydrolysis mechanism. (b) Evolution of the electronic transition's nature of A and B bands during the iodido aquation mechanism (*cis*-$PtI_2(NH_3)_2$ *top*, [*cis*-$PtI(H_2O)(NH_3)_2]^+$ *middle* and [*cis*-$Pt(H_2O)_2(NH_3)_2]^{2+}$ *bottom*): for each transition red densities correspond to arrival orbitals and blue densities correspond to starting molecular orbitals. Platinum ions are coloured in silver, nitrogen in blue, oxygen in red, iodide in violet and hydrogen in white.

ammonia and water molecules. Therefore bands (A) and (B) can be described as I,O($p_{x,y}$) → Pt($d_{x^2-y^2}$) and Pt(d_{xy}) → Pt($d_{x^2-y^2}$) transitions, respectively.

DNA binding properties of *cis*-$PtI_2(NH_3)_2$

To determine the nature of the DNA interactions of *cisPtI*$_2$, the DNA binding properties of this complex were examined through a variety of methods and compared with those of cisplatin. First, we aimed at quantifying the binding of *cisPtI*$_2$ to mammalian (CT) double-helical DNA in a cell free medium.

The amount of platinum bound to DNA increased with time and the times at which the binding reached 50% ($t_{50\%}$) are summarized in Table 1.

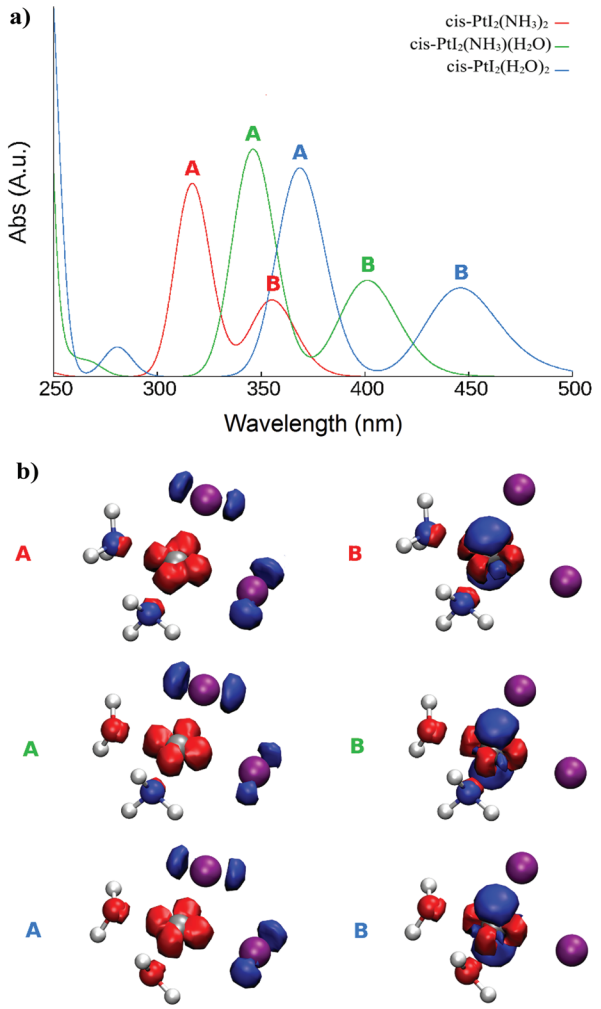

Fig. 5 (a) Evolution of UV-Vis spectral features for the ammonia hydrolysis mechanism. (b) Evolution of the electronic transition's nature of A and B bands during the ammonia aquation mechanism (*cis*-$PtI_2(NH_3)_2$ *top*, [*cis*-$PtI_2(NH_3)(H_2O)$] *middle* and [*cis*-$PtI_2(H_2O)_2$] *bottom*): for each transition red densities correspond to arrival orbitals and blue densities correspond to starting molecular orbitals. Colour code as in Fig. 4.

Table 1 Binding of *cis*-$PtI_2(NH_3)_2$ and cisplatin to calf thymus DNA

Compound	$t_{50\%}$ [a] (min)
cis-$PtI_2(NH_3)_2$ aged in H_2O	105 ± 11
Cisplatin aged in H_2O	64 ± 5
cis-$PtI_2(NH_3)_2$ aged in 10 mM KI	390 ± 24
Cisplatin aged in 10 mM KCl	136 ± 19

[a] The time at which the binding reached 50%. Values shown in the table are the means ± SEM of three separate experiments.

Importantly, after 24 h, *cisPtI*$_2$ and cisplatin aged in water or in 10 mM KI/KCl were quantitatively bound. As expected, the Pt^{II} complexes preincubated in water reacted with DNA significantly more rapidly than those preincubated in KI/KCl (10 mM), but the rate of the reaction of cisplatin was considerably higher than that of *cisPtI*$_2$.

The lower rate of the reaction of *cisPtI*$_2$ with double-helical DNA in comparison with that of cisplatin can be interpreted[35] as the rate of the aquation of the leaving ligands in *cisPtI*$_2$ is significantly lower than that in cisplatin. Since interstrand and intrastrand cross-links formation are believed to be responsible for anticancer activity of bifunctional platinum compounds, we have quantitated the interstrand cross-linking efficiency of *cisPtI*$_2$ in the linear pUC19 DNA (linearized with EcoRI restriction enzyme). Results point out that interstrand cross-linking efficiency of *cisPtI*$_2$ (5 ± 2%) was similar to that of cisplatin (6%) (see ESI† for further details).[32]

Afterwards, to gain more information on the adducts formed in the reaction of *cisPtI*$_2$ with DNA, in comparison with those produced by cisplatin, experiments with the fluorescent probe ethidium bromide have been carried out. Double helical DNA was first modified by the Pt^{II} complex (*cisPtI*$_2$ or cisplatin) for 24 h. The levels of the modification corresponded to the values of r_b in the range between 0 and 0.1. Modification of DNA by both platinum complexes resulted in a decrease of EtBr fluorescence (Fig. 6).

The formation of adducts of *cisPtI*$_2$ resulted in a progressive decrease of EtBr fluorescence intensity, which was similar to that of cisplatin. This result suggests that the conformational distortion induced in DNA by the adducts of *cisPtI*$_2$ is delocalized and extends over the same number of base pairs around the platination sites as in the case of the adducts of cisplatin.

Even the DNA unwinding experiment suggests the same mode of metalation between cisplatin and its iodide analogue (see ESI† for further experimental details). Using this approach, we determined the DNA unwinding angles to be in

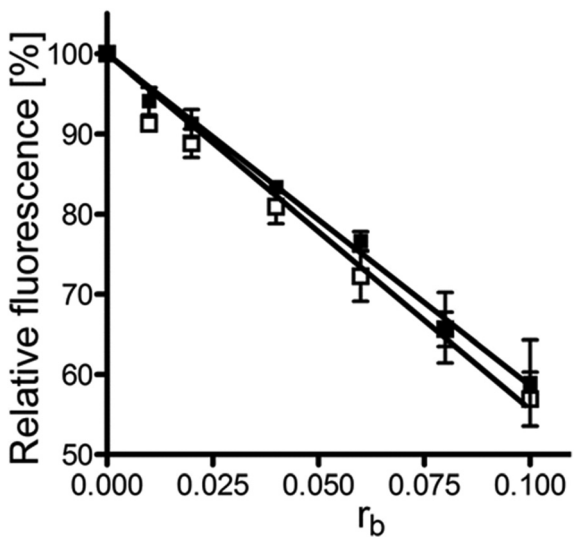

Fig. 6 Ethidium bromide fluorescence. Dependences of the EtBr fluorescence on r_b for CT DNA modified by platinum complexes in 10 mM $NaClO_4$ at 37 °C for 24 h. Open symbols, *cis*-$PtI_2(NH_3)_2$; closed symbols, cisplatin.

Table 2 Δt_m (°C) values[a] of CT DNA modified by *cis*-$PtI_2(NH_3)_2$ or cisplatin[b,c]

	r_b = 0.03	r_b = 0.06	r_b = 0.09
cis-$PtI_2(NH_3)_2$	−1.9 ± 0.1	−5.0 ± 0.1	−7.9 ± 0.3
Cisplatin	−2.1 ± 0.3	−5.2 ± 0.3	−8.3 ± 0.3

[a] Δt_m is defined as the difference between the t_m values of platinated and unmodified DNAs. [b] The t_m values were measured in the medium containing $NaClO_4$ (0.1 M), Tris-HCl (1 mM, pH 7.4) and EDTA (0.1 mM). [c] Values shown in this table are the means ± SEM of three separate experiments.

the range 11 ± 2° for *cisPtI₂*, which is very similar to that found for cisplatin (13°).[30] Finally the thermal stability experiment of DNA has been carried out.

CT DNA was modified by *cisPtI₂* to the value of r_b = 0.03–0.09. After the modification, the salt concentration was further adjusted to 0.1 M by the addition of NaCl, and the samples were further supplemented by Tris-HCl (1 mM) and EDTA (0.1 mM). Thus, the melting curves for DNA modified by the platinum compounds were measured at a relatively high salt concentration (Table 2). We found that the effect of DNA platination by *cisPtI₂* on the melting temperature of DNA (t_m) is similar to that observed for the modifications by cisplatin.

Previously, three major factors have been used to account for the thermal stability of DNA modified by Pt^{II} complexes capable of DNA cross-linking. The observed total change in melting temperature of DNA is a consequence of the relative proportion and contribution of these three factors.[36]

These three factors are (i) a destabilizing effect of conformational distortions due to the formation of cross-links induced in DNA by platinum coordination; (ii) the stabilizing effects of DNA interstrand cross-links which prevent dissociation of DNA strands; (iii) the positive charge on the Pt^{II} centers (introduction of a positive charge into the DNA molecule, *e.g.* by binding of positively charged ligands such as Pt^{II} moieties of platinum compounds, results in a stabilization of the DNA duplex by decreasing the electrostatic repulsion of negative charges of phosphate groups located at the complementary strands).

Thus, it is reasonable to conclude that the decreases in t_m are caused by destabilizing conformational distortions and that these destabilizing factors dominate over the interstrand cross-links formed by both *cis*-platinum compounds and by positive charges on platinum moieties.

Owing to the fact that both *cisPtI₂* and cisplatin carry the same 2+ charge on platinum moiety and form approximately identical amounts of interstrand cross-links (5 or 6%, respectively, *vide supra*), the values of t_m yielded by the adducts of both complexes reflect mainly the destabilizing effects of conformational distortions induced by the platinum–DNA adducts. Hence, the results of DNA melting experiments are consistent with the hypothesis that DNA adducts of *cisPtI₂* distort and destabilize double helix of DNA approximately to the same extent as the DNA adducts of cisplatin.

From overall inspection of the obtained results it is evident that *cisPtI₂* interacts with DNA through a mode of interaction that is very similar to that well documented for cisplatin. Apparently, the major difference consists of a somewhat slower kinetics of platinum association to DNA while the formed adducts are apparently the same.

Cellular actions of *cis*-Pt $I_2(NH_3)_2$

Afterwards, the antiproliferative effects of *cisPtI₂* were evaluated in a representative panel of cancer cell lines according to the method described in the Experimental section.

The cancer cell panel included the following lines: *PANC-1* (human pancreatic cancer), *IGROV-1* (human ovarian cancer), *A549* (human lung cancer), *HT29* (human colon cancer), *HCT116-S* and *HCT116-R* (human colon cancer). These cells were exposed to increasing concentrations of the drugs in the range 0–200 μM; after 24 hours viable cells (determined by Trypan blue exclusion) were counted and the IC_{50} values determined. The measured IC_{50} values are reported in Table 3.

From data inspection it is evident that *cisPtI₂*, in the four cisplatin sensitive cell lines, produces on the whole cytotoxic effects comparable and often greater than cisplatin. Extremely meaningful is the case of IGROV-1 where the cytotoxicity of *cisPtI₂* is far higher than cisplatin (IC_{50} = 7.36 μM *versus* 25.30 μM). Moreover, very remarkably, *cisPtI₂* is found to completely overcome resistance to cisplatin in the cisplatin-resistant HCT116-R line. These results are very relevant and unexpected if one considers that *cisPtI₂* is commonly known to be inactive.

The effects of *cisPtI₂* on the cell cycle were also analysed in HCT116-R cells in comparison with cisplatin; an arrest in the G2/M phase is clearly detected in both cases as well as a decrease of the S phase (Fig. 7).

Analytical determinations were then carried out to measure intracellular Pt content in HCT116-S and HCT116-R cells after exposure to equimolar concentrations of either cisplatin or *cisPtI₂*. More precisely, cells were exposed to a 20 μM concentration of the Pt complexes for 3 h. Results expressed as Pt content per cell in the various cases and as percentage of internalised Pt are reported in Table 4.

From the inspection of Table 4 it is evident that *cisPtI₂* manifests a greater ability to enter both types of cells than cisplatin; such a difference is more evident in the Pt resistant cell line compared to the Pt sensitive one (5 folds *vs.* 2 folds). This

Table 3 IC_{50} values (μM) of cisplatin and its iodo analogue in a panel of cancer cell lines

Cell line	Cisplatin	*cis*-$PtI_2(NH_3)_2$
PANC-1	2.48 ± 0.11	0.91 ± 0.10
IGROV-1	25.30 ± 0.40	7.36 ± 0.31
A549	5.77 ± 0.60	3.54 ± 0.49
HT29	16.39 ± 1.10	11.69 ± 1.40
HCT116-S	7.65 ± 0.63	13.42 ± 0.49
HCT116-R	21.96 ± 1.11	4.15 ± 0.23

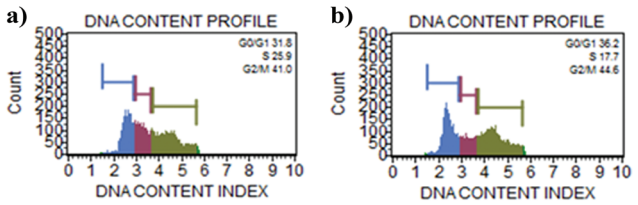

Fig. 7 Cell cycle analysis in HCT116 treated with cisplatin (a) or *cisPtI*$_2$ (b).

Table 4 Platinum level (per cell) measured after exposure (3 hours) of cell lines to 20 μM of cisplatin and *cisPtI*$_2$

Cell line	Drug	Platinum level	Internalised Pt%
HCT116-S	Cisplatin	2.53×10^{-8} μg	0.98
HCT116-S	*cis*-$PtI_2(NH_3)_2$	5.37×10^{-8} μg	1.91
HCT116-R	Cisplatin	1.46×10^{-8} μg	0.50
HCT116-R	*cis*-$PtI_2(NH_3)_2$	6.66×10^{-8} μg	2.41

is possibly linked to its greater lipophilic character and larger inertness.

Furthermore, in the resistant cell line (HCT116-R), we can pinpoint the correlation occurring between the above IC_{50} values and Pt uptake in the sense that a greater cytotoxicity is associated with a greater Pt uptake – in terms of a five fold difference – proving the capability of *cisPtI*$_2$ to overcome chemo-resistance.

Discussion and conclusions

The substantial lack of information concerning *cisPtI*$_2$ despite its striking similarity to cisplatin has inspired the present study; notably, some crucial aspects of its chemical and biological profile have been eventually elucidated.

First, we have shown that *cisPtI*$_2$ manifests a solution behaviour very similar to cisplatin when dissolved in an aqueous medium, at physiological pH; indeed, as seen for cisplatin, *cisPtI*$_2$ undergoes activation through sequential slow release of its two iodido ligands that are replaced by water molecules. However, the process is appreciably slower than in the case of cisplatin. These statements are clearly supported both by experimental data (see the ESI†) and computational analysis. The alternative hydrolysis path, where preferential release of NH_3 ligands is observed, could also be induced by changing the pH conditions. Even in this latter case the reaction route has been characterized by spectrophotometric analysis and spectral simulations. The large differences observed between the spectral patterns associated with the two possible mechanisms are very consistent with our interpretation.

Then, the reactions of *cisPtI*$_2$ with DNA were investigated in detail in direct comparison with cisplatin through a robust experimental approach involving a variety of independent biophysical methods. Remarkably, we found that the pattern of DNA platination produced by *cisPtI*$_2$ is highly reminiscent and nearly superimposable to that of cisplatin though the kinetics of the DNA metalation process is again appreciably slower.

Afterwards, the cellular effects induced by *cisPtI*$_2$ were explored in a small but representative panel of solid tumor cell lines; the panel included PANC-1 (human pancreatic cancer), IGROV-1 (ovarian cancer), A549 (lung cancer), HT29 (colon cancer), HCT116-S (colon cancer) and HCT116-R cells. Very remarkably, we observed that *cisPtI*$_2$, in contrast to expectations and to the current opinion, is on the whole more cytotoxic than cisplatin in three out of four cisplatin sensitive cancer cells; on the other hand, *cisPtI*$_2$ was found to completely overcome resistance to cisplatin in the cisplatin resistant HCT116-R cell line. This latter result implies that *cisPtI*$_2$ is able to circumvent the molecular mechanisms that reduce sensitivity to cisplatin in the resistant line. On the other hand, it is unlikely that dimeric Pt species (see the ESI†) play a major role in the observed cytotoxicity as the latter species are detected only at acidic pH and in very low amounts.

Analytical determinations were carried out to measure Pt uptake in the various cases: we found that cisplatin manifested a far lower ability to enter cells than *cisPtI*$_2$. In addition, a pronounced reduction of Pt uptake was detected in HCT116 resistant cells in comparison with their sensitive counterparts upon cisplatin treatment implying that this is most likely the main mechanism of resistance. In contrast, *cisPtI*$_2$ is internalised in far greater amounts by both cell types with resistant cells even showing a slightly greater Pt uptake.

However, the correlation between the cytotoxic potency and the intracellular Pt content is not straightforward for both HCT116 cellular lines. For instance, the Pt content measured upon exposure of HCT116-S cells to *cisPtI*$_2$ is more than two times greater compared with exposure to cisplatin. Yet, cisplatin produces a greater cytotoxic effect than *cisPtI*$_2$ (by a factor 2). Pairwise, roughly comparable amounts of intracellular Pt are found in HCT116-R and HCT116-S cells upon exposure to *cisPtI*$_2$; but *cisPtI*$_2$ is far more cytotoxic in the resistant cells compared to the sensitive ones (by a factor 3). This implies that the nature of the cells and the nature of the Pt complex are still important in determining the overall antiproliferative effect.

We believe that the here reported results are very meaningful and innovative with respect to the current mechanistic knowledge on cisplatin and on its analogues for the following reasons:

1. In contrast to expectations and to early claims of inactivity *cisPtI*$_2$ is found to produce cytotoxic effects comparable and often greater than those caused by cisplatin, at least in four representative cancer cell lines;

2. *cisPtI*$_2$ overcomes to a large extent resistance to cisplatin in a cancer cell line showing acquired resistance to cisplatin, being taken up in a far greater amount. This implies that the recognition processes for the two Pt complexes are distinct.

3. However, the large differences measured in Pt uptake between *cisPtI*$_2$ and cisplatin do not correlate with the large differences observed in their respective biological effects. The

nature of the Pt complex and the type of cell still play major roles.

4. The aquation process of *cisPtI*$_2$ at physiological pH reproduces closely that of cisplatin – though being slower – involving the progressive release of the two halide ligands; however, at slightly acidic pH, *cisPtI*$_2$ is found to release preferentially its ammonia ligands at variance with cisplatin. These processes are reproduced very satisfactorily through computational analysis of the respective spectral profiles. It is very likely that these differences in reactivity between *cisPtI*$_2$ and cisplatin may lead to different interaction modes with specific biomolecules, in particular with proteins, thus generating distinct pharmacological profiles.

5. Remarkably, *cisPtI*$_2$ produces a kind of DNA damage very similar to cisplatin. Yet, the kinetics of Pt binding to DNA is slower and the final level of DNA platination is appreciably lower. As the process of DNA platination is apparently less efficient than in the case of cisplatin it is unlikely that DNA is the only or primary target for *cisPtI*$_2$, when one considers that *cisPtI*$_2$ is even more cytotoxic than cisplatin.

Altogether, the reported results delineate an extremely favourable biological profile for *cisPtI*$_2$ and strongly warrant its further assessment in appropriate preclinical models. Moreover, at least in our opinion, these findings contain relevant implications with respect to the postulated mode of action of cisplatin and of its analogues. As DNA damage produced by *cisPtI*$_2$ is, on the whole, less extensive and less important than that induced by cisplatin and the type of DNA lesion is basically the same, the view that the cytotoxic effects of *cisPtI*$_2$ may arise from mechanisms other than DNA damage is supported. However, more studies are definitely needed to further substantiate this hypothesis.

Acknowledgements

TM and LM acknowledge Beneficentia Stiftung (Vaduz), COST Action CM1105 and AIRC (IG-16049) for generous financial support. JK and VB acknowledge the support from the Czech Science Foundation (Grant 14-21053S).

Notes and references

1 D. Wang and S. J. Lippard, *Nat. Rev. Drug Discovery*, 2005, **4**, 307.
2 Z. H. Siddik, *Oncogene*, 2003, **22**, 7265.
3 L. Kelland, *Nat. Rev. Cancer*, 2007, **7**, 573.
4 E. Raymond, S. Faivre, S. Chaney, J. Woynarowski and E. Cvitkovic, *Mol. Cancer Ther.*, 2002, **1**, 227.
5 A. M. Florea and D. Büsselberg, *Cancers*, 2011, **3**, 1351.
6 O. Rixe, W. Ortuzar, M. Alvarez, R. Parker, E. Reed, K. Paull and T. Fojo, *Biochem. Pharmacol.*, 1996, **52**, 1855.
7 A. Casini and J. Reedijk, *J. Chem. Sci.*, 2012, **3**, 3135.
8 O. Pinato, C. Musetti and C. Sissi, *Metallomics*, 2014, **6**, 380.
9 G. Natile and M. Coluccia, in *Metal Ions in Biological Systems*, ed. A. Sigel and H. Sigel, Marcel Dekker Inc., New York, 2004, vol. 42, p. 209.
10 M. Galanski, A. Yasemi, S. Slaby, M. A. Jakupec, V. B. Arion, M. Rausch, A. A. Nazarov and B. K. Keppler, *Eur. J. Med. Chem.*, 2004, **39**, 707.
11 (*a*) J. J. Wilson and S. J. Lippard, *Chem. Rev.*, 2014, **114**, 4470; (*b*) T. M. Johnstone, G. Y. Park and S. J. Lippard, *Anticancer Res.*, 2014, **34**, 471; (*c*) T. C. Johnstone, K. Suntharalingam and S. J. Lippard, *Philos. Trans.: Math., Phys. Eng. Sci.*, 2015, **373**, 20140185.
12 M. D. Hall, H. R. Mellor, R. Callaghan and T. W. Hambley, *J. Med. Chem.*, 2007, **50**, 3403.
13 M. S. Davies, D. S. Thomas, A. Hegmans, S. J. Berners-Price and N. Farrel, *Inorg. Chem.*, 2002, **41**, 1101.
14 (*a*) M. J. Cleare and J. D. Hoeschele, *Bioinorg. Chem.*, 1973, **2**, 187; (*b*) K. Nakamoto, *Infrared and Raman Spectra of Inorganic and Coordination Compounds, Part B. Application in Coordination, Organometallic and Bioinorganic Chemistry*, Wiley Interscience, John Wiley and Sons, Inc., New York, 5th edn, 1997, ISBN 0-471-16392-9; (*c*) F. D. Rochon and V. Buculei, *Inorg. Chim. Acta*, 2004, **357**, 2218.
15 N. A. Kratochwil, A. I. Patriarca, J. A. Parkinson, A. M. Gouldsworthy and P. D. S. Murdoch, *J. Am. Chem. Soc.*, 1999, **36**, 8193.
16 L. Messori, L. Cubo, C. Gabbiani, A. Álvarez-Valdés, E. Michelucci, G. Pieraccini, C. Ríos-Luci, J. M. Padron, C. Navarro-Ranninger, A. Casini and A. G. Quiroga, *Inorg. Chem.*, 2012, **51**, 1717.
17 L. Messori, A. Casini, C. Gabbiani, E. Michelucci, L. Cubo, C. Ríos-Luci, J. M. Padron, C. Navarro-Ranninger and A. G. Quiroga, *ACS Med. Chem. Lett.*, 2010, **1**, 381.
18 T. Parro, M. A. Medrano, L. Cubo, S. Muñoz-Galván, A. Carnero, C. Navarro-Ranninger and A. G. Quiroga, *J. Inorg. Biochem.*, 2013, **127**, 182.
19 L. Messori, T. Marzo, C. Gabbiani, A. A. Valdes, A. G. Quiroga and A. Merlino, *Inorg. Chem.*, 2013, **52**, 13827.
20 S. C. Dhara, *Indian J. Chem.*, 1970, **8**, 193.
21 F. Neese, *Wiley Interdiscip. Rev.: Comput. Mol. Sci.*, 2012, **2**, 73.
22 J. P. Perdew, M. Ernzerhof and K. Burke, *J. Chem. Phys.*, 1996, **105**, 9982.
23 D. A. Pantazis, X. Y. Chen, C. R. Landis and F. Neese, *J. Chem. Theor. Comput.*, 2008, **4**, 908.
24 E. Runge and E. K. Gross, *Phys. Rev. Lett.*, 1984, **52**, 997.
25 S. Grimme, J. Antony, S. Ehrlich and H. Krieg, *J. Chem. Phys.*, 2010, **132**, 154104.
26 A. Klamt and G. Schiiiirmann, *J. Chem. Soc., Perkin Trans. 2*, 2993, 799.
27 S. Sinnecker, A. Rajendran, A. Klamt, M. Diedenhofen and F. Neese, *J. Phys. Chem. A*, 2006, **110**, 2235.
28 M. V. Baker, P. J. Barnard, S. J. Berners-Price, S. K. Brayshaw, J. L. Hickey, B. W. Skelton and A. H. White, *Dalton Trans.*, 2006, 3708.
29 S. D. Kim, O. Vrana, V. Kleinwächter, K. Niki and V. Brabec, *Anal. Lett.*, 1990, **23**, 1505.

30 M. V. Keck and S. J. Lippard, *J. Am. Chem. Soc.*, 1992, **114**, 3386.
31 N. Farrel, Y. Qu, L. Feng and B. Van Houten, *Biochemistry*, 1990, **29**, 9522.
32 V. Brabec and M. Leng, *Proc. Natl. Acad. Sci. U. S. A.*, 1993, **90**, 5345.
33 J. L. Butour, P. Alvinerie, J. P. Souchard, P. Colson, C. Houssier and N. P. Johnson, *Eur. J. Biochem.*, 1991, **202**, 975.
34 (*a*) F. D. Rochon and P. C. Kong, *Inorg. Chim. Acta*, 1986, **64**, 1894; (*b*) J. Zhang, L. Liu, Y. Gong, X. Zheng, M. Yang, J. Cui and S. Shen, *Eur. J. Med. Chem.*, 2009, **44**, 2322.
35 H. Kostrhunova, O. Vrana, T. Suchankova, D. Gibson, J. Kasparkova and V. Brabec, *Chem. Res. Toxicol.*, 2010, **23**, 1833.
36 R. Zaludova, V. Kleinwächter and V. Brabec, *Biophys. Chem.*, 1996, **60**, 135–142.